Weakly Supervised Anomaly Detection via Knowledge-Data Alignment

Haihong Zhao
Hong Kong University of Science and Technology (Guangzhou)
Guangzhou, China
hzhaobf@connect.ust.hk

Chenyi Zi
Hong Kong University of Science and Technology (Guangzhou)
Guangzhou, China
czi447@connect.hkust-gz.edu.cn

Yang Liu
Hong Kong University of Science and Technology
Hong Kong, China
yliukj@connect.ust.hk

Chen Zhang
CreateLink Technology
China
zhangchen@chuanglintech.com

Yan Zhou
CreateLink Technology
China
zhouyan@chuanglintech.com

Jia Li[*]
Hong Kong University of Science and Technology (Guangzhou)
Guangzhou, China
jialee@ust.hk

ABSTRACT

Anomaly detection (AD) plays a pivotal role in numerous web-based applications, including malware detection, anti-money laundering, device failure detection, and network fault analysis. Most methods, which rely on unsupervised learning, are hard to reach satisfactory detection accuracy due to the lack of labels. Weakly Supervised Anomaly Detection (WSAD) has been introduced with a limited number of labeled anomaly samples to enhance model performance. Nevertheless, it is still challenging for models, trained on an inadequate amount of labeled data, to generalize to unseen anomalies. In this paper, we introduce a novel framework Knowledge-Data Alignment (KDAlign) to integrate rule knowledge, typically summarized by human experts, to supplement the limited labeled data. Specifically, we transpose these rules into the knowledge space and subsequently recast the incorporation of knowledge as the alignment of knowledge and data. To facilitate this alignment, we employ the Optimal Transport (OT) technique. We then incorporate the OT distance as an additional loss term to the original objective function of WSAD methodologies. Comprehensive experimental results on five real-world datasets demonstrate that our proposed KDAlign framework markedly surpasses its state-of-the-art counterparts, achieving superior performance across various anomaly types.

CCS CONCEPTS

• **Information systems** → **Anomaly Detection; Web mining**; • **Computing methodologies** → **Neural networks**.

---

[*] Corresponding author.

KEYWORDS

Anomaly Detection; Knowledge-Data Alignment; Weakly Supervised Learning

1 INTRODUCTION

Anomaly detection (AD), aiming at identifying patterns or instances that deviate significantly from the expected behavior or normal patterns, is crucial to extensive web-based applications including malware detection [31], anti-money laundering [35], device failure detection [55], network fault analysis [27, 73]. Given that labeled anomaly data is typically scarce or costly to acquire, unsupervised methodologies that operate on entirely unlabeled data have gained widespread use. However, in the absence of supervision, these models may incorrectly classify noisy or unrelated data as anomalies, leading to high detection errors.

To alleviate the above issue, Weakly Supervised Anomaly Detection (WSAD) has been proposed to enhance detection accuracy with limited labeled anomaly samples and a large amount of unlabeled data [29], shown in Fig. 1(a). Early studies use unsupervised AD algorithms as feature extractors and learn a supervised classifier with label data [26, 40, 45, 54, 58, 63]. With the development of deep learning, most recent studies focus on end-to-end frameworks that build on multilayer perceptron, autoencoder, and generative adversarial networks, to directly map input data to anomaly scores [1, 36, 48, 74]. Nevertheless, models trained on insufficient labeled data fail to generalize to novel anomalies or anomalies not observed during training time [28, 29]. Although several works have employed active learning or reinforcement learning to reduce the cost of obtaining anomaly labels, they still require an initial set of labeled data to start the learning process, which can be costly and time-consuming [38, 70].

In this work, we propose to incorporate rule knowledge, which is often derived or summarized by human experts [7, 39, 42, 68, 73],

Haihong Zhao, Chenyi Zi, Yang Liu, Chen Zhang, Yan Zhou, and Jia Li[*]
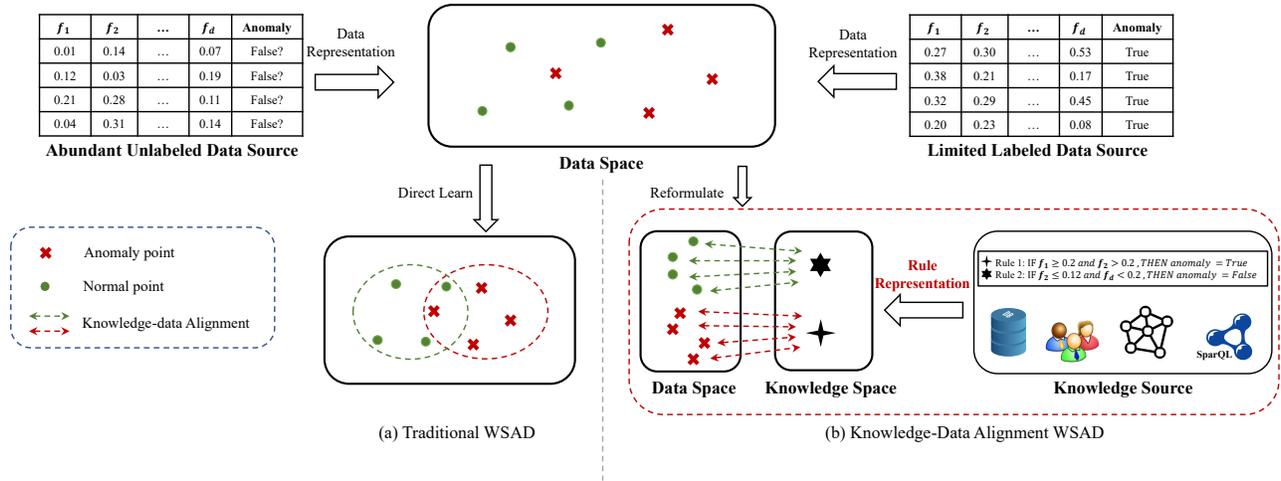
Figure 1: Comparison between traditional WSAD approach (a) and our proposed knowledge-data alignment WSAD framework (KDAlign) (b). We can find that the traditional WSAD mainly focuses on learning from limited labeled data, while our proposed framework introduces knowledge as extra information to supplement limited labeled via knowledge-data alignment. Note that the samples in the unlabeled data source are usually regarded as normal samples, though the unlabeled data may be contaminated by noise [28, 46].

similar to label annotation but has been largely overlooked, to help complement the limited labeled data, as shown in Fig. 1(b). Although rules are high-quality and accessible in practice [39, 42], incorporating them is non-trivial for three reasons: (1) knowledge representation: rules are generally represented by if/else statements [39, 42]. In the representation space, rules and data lack a direct correlation [66, 73], making them unsuitable for directly training the WSAD models; (2) knowledge-data alignment: intuitively, if two rules are close then their corresponding data samples should be also close [7]. For example, in anti-money laundering, a group of fraudsters may possess similar patterns and thus have similar data representations [7, 39, 42]. Usually, these fraudsters will be detected by identical or similar if/else rule statements in anti-money laundering systems [7]. In this work, we reformulate the knowledge incorporation process as the knowledge-data alignment and supplement the traditional data-only optimizations; (3) noisy knowledge: typically, rules are not always accurate [4, 7, 39], thus directly aligning them with data may involve noises and resulting in a performance drop. It is still challenging to ensure the model's performance under noisy rules.

To address the above issues, we propose a novel framework for Weakly Supervised Anomaly Detection via **K**nowledge-**D**ata **Align**ment (**KDAlign**). KDAlign expects to align knowledge and data to complement the data distribution. For the first challenge, KDAlign employs a knowledge encoder to map the rules into an embedding space, thereby allowing knowledge to correlate with data in the numerical domain. For the second and third challenges, KDAlign leverages the Optimal Transport (OT) technique to align knowledge and data. The primary strength of OT lies in its inherent flexibility. It autonomously determines the optimal transport pairings between knowledge and data, thus establishing an intrinsic

connection [44, 61, 62, 72]. Specifically, the OT method intrinsically forms a robust framework, enabling a geometrically faithful comparison of probability distributions and facilitating the information transfer between distinct distributions [22]. Regarding noisy knowledge, when a sample matches a noisy rule, the distance of that sample to some other closely related rules will be farther, resulting in an increased OT distance penalty. To ensure global optimality, the OT distance between this sample and the noisy rule will be constrained by other correct rules, thereby ensuring the performance of KDAlign.

To sum up, our contributions are three-fold:

- To the best of our knowledge, this is the first work to incorporate rule knowledge into WSAD, effectively complementing the limited labeled data.
- We propose a novel Knowledge-Data Alignment Weakly Supervised anomaly detection framework (KDAlign).
- The experimental results on five public WSAD datasets indicate our proposed KDAlign are superior to all the competitors. Furthermore, KDAlign achieves strong performance improvements even with 20% noisy rule knowledge.

2 PRELIMINARY

2.1 Rule Knowledge and Logical Formulae

In this paper, we focus on rule knowledge (if/else). This choice stems from the high-quality and accessible in practice of rules — they present explicit conditions and outcomes. Such transparency allows individuals to understand anomaly and normal data easily. To avoid the potential overlaps among different rules, we adopt a precise knowledge statement format named Logical Formulae. Concretely, logical statements provide a flexible declarative language for expressing structured knowledge (e.g., rule knowledge). In this paper,
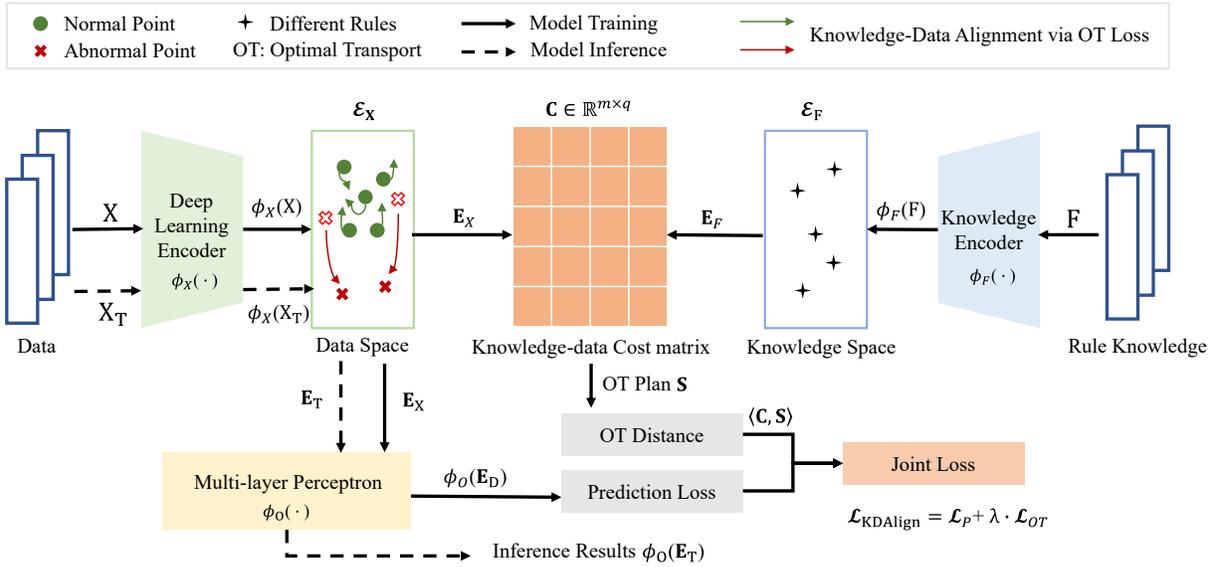
Figure 2: Knowledge-data alignment WSAD framework. During the training phase, we firstly use ϕ_X and ϕ_F to map X and F to two separate embedding spaces and then leverage Optimal Transport (OT) techniques to compute the cost matrix C, thereby obtaining the OT plan S. Next, we compute OT distance $\langle C, S \rangle$ and add it as a loss term to the prediction loss term, forming a joint loss. Finally, we utilize the joint loss to train $\phi_X(\cdot)$ and $\phi_O(\cdot)$, aligning knowledge and data for incorporating knowledge. In the inference phase of the model, the test data directly yields results by ϕ_X and ϕ_O. In the data space, both the abnormal and normal points can be aligned via OT.

we focus on **propositional logic**, where a **proposition** p is a statement which is either **True** or **False** [34]. A statement (proposition) consists of a subject, predicate and object. It can also be regarded as a ground clause that does not contain any variables [17]. A **propositional formula** f is a compound of propositions connected by logical connectives [8, 66], e.g., $\neg$, $\wedge$, $\vee$, $\Rightarrow$. Also, a propositional formula is equal to a grounding first-order logic formula. In the subsequent content, we use $F = \{f_1, \ldots, f_s\}$ to represent a set of propositional formulae, where f_i is a propositional formula and s is the number of propositional formulae. The concrete proposition formats designed for rule knowledge of AD are introduced in Section 3.

2.2 Problem Statement

Given a training dataset $X = \{x_1, x_2, \cdots, x_n, x_{n+1}, \cdots, x_{n+m}\}$, with $x_i \in \mathbb{R}^d$, where $X_U = \{x_1, x_2, \cdots, x_n\}$ is a large unlabeled dataset and $X_A = \{x_{n+1}, x_{n+2}, \cdots, x_{n+m}\}$ $(m \ll n)$ is a small set of labeled anomaly examples that often can not cover every possible class of anomaly, a WSAD model $\mathcal{M}$ is first trained on X to output anomaly score $O := \mathcal{M}(X) \in \mathbb{R}^{m \times 1}$, where higher scores indicate a higher likelihood of an abnormal sample. The unlabeled dataset X_U is usually assumed as normal data, though it may be contaminated by some anomalies in practice [46, 47]. Thus, the trained $\mathcal{M}$ is required to be robust *w.r.t.* such anomaly contamination. Based on the trained model, we need to predict on the unlabeled test dataset $X_T \in \mathbb{R}^{q \times d}$, so to return $O_T := \mathcal{M}(X_T) \in \mathbb{R}^{q \times 1}$. In our work, we introduce a set of rule knowledge represented by propositional formulae F, as extra information, to supplement data and then training a WSAD models on $\{X, F\}$.

3 METHODOLOGY

3.1 Overview

Figure 2 provides an overview of our proposed **K**nowledge-**D**ata **Align**ment WSAD framework (**KDAlign**). First, we utilize a deep learning encoder and a knowledge encoder to project data X and knowledge F into data embedding space $\mathcal{E}_X$ and knowledge embedding space $\mathcal{E}_F$, respectively, making operations between knowledge and data possible. The deep learning encoder could be based on a multi-layer perceptron, autoencoder, or ResNet-like architecture. The knowledge encoder is a multi-layer graph convolutional network. Second, within the embedding space, we align data and knowledge via the Optimal Transport Technique (OT) and then leverage the alignment result to derive an OT loss term. The OT loss term is subsequently used for introducing the knowledge into deep learning models. Besides, we give an analysis of why KDAlign has the potential to alleviate the noisy knowledge issue. Third, we jointly leverage the OT loss and the prediction loss to train a deep-learning model, expecting to learn better data representations for X and improve the model performance, where the original loss is computed by the output of the multi-layer perceptron and labels. Then, the trained model can be used for inferring unlabeled test data.

3.2 Representation Framework

3.2.1 Data Representation. Given the training dataset X with m samples, we use a deep learning encoder to project data into a high-dimensional embedding space, generating the corresponding

data embedding set $E_X = \{e_1, \ldots, e_m\}$, where m is the number of samples. The process is shown by Equation 1

$$E_X = \phi_X(X) \in \mathbb{R}^{m \times h}, \tag{1}$$

where ϕ_X is a deep learning encoder, and h is the dimension of the Data Space $\mathcal{E}_X$ defined by E_X.

3.2.2 *Knowledge Representation*.
In order to enable knowledge and data to be operated, we also consider representing knowledge in a high-dimensional embedding space, but embedding knowledge successfully entails rendering it into a format amenable for processing by deep learning methods. Given s if/else statements, we first contemplate transforming their formats into propositional logic and then generate a knowledge set F with s propositional formulae, which is drawn inspiration from knowledge embedding of logical formulae [65].

Next, we provide an example to illustrate how to transform the if/else statement into propositional logic: Given an if/else statement 'If $attr_1 > 5$ and $attr_2 = 0$, then anomaly is $True$', where $attr_1$ and $attr_2$ correspond to two attributes of the sample, three propositions $\{p_1 = (attr_1 > 5), p_2 = (attr_2 = 0), p_3 = (anomaly\ is\ True)\}$ and a proposition formula $f = \{p_1 \wedge p_2 \Rightarrow p_3\}$ can be generated. The subject, object, and predicate constituting the three propositions are, respectively, $subject = \{attr_1, attr_2, anomaly\}$, $object = \{5, 0, True\}$, $predicate = \{>, =, is\}$.

Building upon the example above, we provide definitions for the subject, object, and predicate in propositional formulae used to describe if/else statements: The subject comprises attribute names present in the sample and the word 'anomaly'; the object encompasses attribute thresholds, words 'True', and 'False'; the predicate consists of numeric relational symbols and the word 'is'.

Based on the transformation strategy, we convert if/else statements into a set of propositional formulae $F = \{f_1, \ldots, f_s\}$. Subsequently, each propositional formula in F is transformed into a graph structure, and then a multi-layer graph convolutional network [65] is constructed as a knowledge encoder to project propositional formulae into a high-dimensional embedding space named Knowledge Space and generate the knowledge embedding set $E_F = \{e_1, \ldots, e_s\}$, where s is the number of propositional formulae, shown in Equation 2

$$E_F = \phi_F(F) \in \mathbb{R}^{s \times h}, \tag{2}$$

where $\phi_F(\cdot)$ is a multi-layer graph convolutional network, and h is the dimension of the Knowledge Space $\mathcal{E}_F$ defined by E_F. Since the dimensions of $\mathcal{E}_F$ and E_X are both h, knowledge and data lie in the same dimensional space. Additionally, $\phi_F(\cdot)$ is trained before the training of the deep learning model ϕ_X. The details of the knowledge encoder are shown in the appendix.

3.3 Knowledge-Data Alignment

3.3.1 *Definition*.
Given a knowledge set F and a limited labeled training dataset X, without any observed knowledge-data correspondences, the alignment algorithm returns aligned knowledge-data pairs $M = \{(f_i, x_j) | (f_i, x_j) \in F \times X\}$.

3.3.2 *Optimal Transport*.
To resolve knowledge-data alignment, we leverage the OT technique that has been widely applied in

various domains for alignment, such as in image and graph domains [3, 61, 64, 71]. We follow the Kantorovich formulation [21, 69], which can be formally defined in terms of two distributions and a cost matrix as follows

Definition 3 (Optimal Transport). Given two sets of observations $O_1 = \{o_1, \ldots, o_{n_1}\}, O_2 = \{o_1, \ldots, o_{n_2}\}$, there are two discrete distributions μ, v defined on probability simplex Δ_1, Δ_2, where n_1 is the number of O_1, and n_2 is the number of O_2. Then, a cost matrix $C \in \mathbb{R}^{n_1 \times n_2}$ is computed for measuring the distance between all pairs $(f_i, x_j) \in \Delta_1 \times \Delta_2$ across two distributions. The OT problem aims to find an OT plan $S \in \Pi(\mu, v)$ between μ and v that minimizes the expected cost over the coupling as follows:

$$\min_{S \in \Pi(\mu, v)} \sum_{f_i, x_j} C(f_i, x_j) S(f_i, x_j) = \min_{S \in \Pi(\mu, v)} \langle C, S \rangle,$$

$$\text{s.t.} \quad S(f_i, x_j) \geq 0, \ for\ all\ i\ and\ j, \tag{3}$$

$$\sum_{i=1}^{n_1} S(f_i, x_j) = \mu_i, \sum_{j=1}^{n_2} S(f_i, x_j) = v_j,$$

where S is the OT plan, $\Pi(\mu, v)$ is the probabilistic coupling between μ and v (i.e., all the available transport plan between μ and v), $\langle \cdot, \cdot \rangle$ is inner product, and corresponding $\langle C, S \rangle$ is the Wasserstein distance between μ and v. In this paper, to efficiently solve the OT problem, we employ the Sinkhorn-Knopp algorithm [11, 21]. The objective of the Sinkhorn-Knopp algorithm is to approximate the computation of the Wasserstein distance, enabling efficient computation of Wasserstein distance, particularly in high-dimensional or large-scale scenarios.

In knowledge-data alignment, we regard μ as the knowledge distribution defined by F and v as the data distribution defined by X, and then $S(f_i, x_j)$ indicates the matching score between f_i in the knowledge set F and x_j in X. The alignment M can be derived from S:

$$M = \arg\max_{M \in \mathbb{M}} \sum_{(f_i, x_j) \in M} S(f_i, x_j), \tag{4}$$

where $\mathbb{M}$ is the set of all legit alignments, $i = 1, \ldots, s$, and $j = 1, \ldots, m$.

3.3.3 *OT Loss For Weakly Supervised Anomaly Detection*.
Obtaining the knowledge-alignment results, we further describe how to utilize the alignment results to benefit WSAD. Firstly, we compute the knowledge-data cost matrix $C \in \mathbb{R}^{s \times m}$ for measuring the distance between all pairs $(\phi_F(f_i), \phi_X(x_j)) \in \mathcal{E}_F \times \mathcal{E}_X$ across two distribution spaces, which describes the discrepancy between the data embeddings and the knowledge embeddings. Secondly, we can compute the OT plan S and the knowledge-data alignment M by Equations 3 and 4, respectively. Thirdly, we also compute the OT distance, which quantifies the minimum cost required to transform one probability distribution into another, by $\langle C, S \rangle$. Finally, the OT distance is used for training the deep learning model.

Analysis On Noisy Knowledge Alleviation. Firstly, we need to clarify the effects of noisy rules on WSAD. Since rules and data are matched one-to-one, when noisy rules emerge, it directly leads to detection errors. We would naturally assume that introducing noisy rule information into data embeddings can also impact the performance of the WSAD model. However, benefiting from the

OT technique, which takes a global perspective to align rules and data, our proposed KDAlign framework would not be obviously influenced by noisy rules. This is because introducing too much noisy rule information can lead to excessive transport distances between the data and other relevant rules, resulting in a suboptimal transport plan. Therefore, to provide the optimal transport plan, the incorporation of noisy rule knowledge is constrained by other correct rules, thereby alleviating the impact of noisy knowledge.

3.4 Model Training and Inference

Model Training. In addition to deep learning encoders for embedding data, we also employ a multi-layer perceptron (MLP) $\phi_O(\cdot)$ to output anomaly scores or classification results based on data embeddings. During the training process, to effectively leverage alignment results, we introduce the OT distance between knowledge and data as a loss term $\mathcal{L}_{OT}$ added to the prediction loss function $\mathcal{L}_P$ computed by output and sample labels, rather than as a regularization term. This is mainly because the OT distance calculated by the Sinkhorn-Knopp algorithm is differentiable. Concretely, this addition introduces an auxiliary objective that allows both the deep learning encoder and MLP to simultaneously update parameters based on $\mathcal{L}_P$ and $\mathcal{L}_{OT}$, effectively incorporating knowledge information into data embeddings. The joint loss function $\mathcal{L}_{KDAlign}$ is shown by Equation 5

$$\mathcal{L}_{KDAlign} = \mathcal{L}_P + \lambda \cdot \mathcal{L}_{OT}, \tag{5}$$

where $\mathcal{L}_P$ is the prediction loss, and $\mathcal{L}_{OT}$ is computed by $\langle \mathbf{C}, \mathbf{S} \rangle$, and λ is the trade-off factor of $\mathcal{L}_{OT}$. From another perspective, the OT loss offers a targeted optimization direction, thereby effectively incorporating knowledge information and enhancing the model performance. In addition, the prediction loss could also be alternated by other losses for AD (e.g., deviation loss [48] and the specially designed deviation loss [74].

Model Inference. The trained deep learning encoder ϕ_X and MLP ϕ_O comprise the WSAD model $\mathcal{M}$, which is used for inference on test dataset by Equation 6

$$\mathcal{M}(\mathbf{X_T}) = \phi_O(\phi_X(X_T)). \tag{6}$$

where ϕ_X is the trained deep learning encoder, ϕ_O is the trained MLP, $\mathcal{M}$ is the trained WSAD model, and X_T is the test dataset.

4 EXPERIMENTS

In this section, we study the experimental results of our proposed method and baselines to answer three research questions:

- **RQ1.** How effective is the proposed KDAlign framework that incorporates knowledge compared with representative baselines in WSAD?
- **RQ2.** How important is the Knowledge-data Alignment in KDAlign?
- **RQ3.** How does noisy knowledge impact the KDAlign?

Table 1: Data description of five datasets used in our experiments. Rule-Detect denotes the number of samples that match rules. Rate is computed by #Rule-Detect/#Label.

Name	Size	#Feature	#Rule	#Label	#Rule-Detect	Rate(%)
Amazon	11944	25	20	821	431	52.0
Cardiotocography	2114	21	14	466	281	60.0
Satellite	6435	36	23	2036	1015	50.0
SpamBase	4207	57	21	1679	968	58.0
YelpChi	45954	32	88	6678	1475	22.0

4.1 Experimental Setup

Datasets. We conduct experiments on five real-world datasets [24, 28, 59]. The **YelpChi** dataset[52, 60] is used for finding anomalous reviews which unjustly promote or demote certain products or businesses on Yelp.com. The **Amazon** dataset[43, 60] seeks to identify the anomalous users paid to write fake product reviews under the Musical Instrument category on Amazon.com. The **Cardiotocography** dataset[2] targets to detect the pathologic fetuses according to fetal cardiotocographies. The **Satellite** dataset [57] is collected for distinguishing anomalous satellite images according to multi-spectral values of pixels in 3x3 neighbourhoods. The **SpamBase** dataset[25] is leveraged to decide spam e-mails on e-mail systems. The descriptions of the five datasets are shown in Table 1.

Metrics. We choose two widely used metrics to evaluate the performance of all the methods[18, 24, 59], namely **AUPRC (Area Under the Precision-Recall Curve)**, and **Rec@K (Recall at k)**. AUPRC is the area beneath the Precision-Recall curve at different thresholds. **AUPRC** can be calculated by the weighted mean of precisions at each threshold, where the increase in recall from the previous threshold serves as the weight. **Rec@K** is determined by calculating the recall of the true anomalies among the top-k predictions that the model ranks with the highest confidence. We set the value of k as the number of actual outliers in the test dataset. It is noteworthy that in this specific scenario, Rec @K is equivalent to both precision at k and the F1 score at k (**F1@K**).

Baselines. We compare the proposed method with the following baselines and give brief descriptions. The first three are typical AD methods. The rest of them are representative of WSAD methods.

- **k-Nearest Neighbors (KNN)** [10]. A classification method based on the k nearest neighbors in the training set.
- **Support Vector Machine (SVM)** [9]. A classification method based on maximum margin.
- **Decision Tree (DT)** [6]. A classification method based on tree structure, and every decision path define an if/else statement.
- **DeepSAD** [54]. A deep semi-supervised one-class method that enhances the unsupervised DeepSVDD.
- **REPEN** [45]. A neural network based model that utilized transformed low-dimensional representation for random distance based detectors.
- **DevNet** [48]. A neural network based model trained by deviation loss.
- **PReNet** [47]. A neural network based model that defines a two-stream ordinal regression to learn the relation of instance pairs.

Haihong Zhao, Chenyi Zi, Yang Liu, Chen Zhang, Yan Zhou, and Jia Li[*]

Table 2: Performance comparison between representative baselines and KDAlign w.r.t. AUPRC and F1@K. The best results are in bold.

Model	Amazon		Cardio		Satellite		SpamBase		YelpChi	
	PRC	F1@K	PRC	F1@K	PRC	F1@K	PRC	F1@K	PRC	F1@K
KNN	0.074	0.071	0.370	0.333	0.326	0.359	0.419	0.406	0.145	0.151
SVM	0.127	0.013	0.654	0.570	0.312	0.296	0.357	0.283	0.130	0.114
DT	0.078	0.065	0.261	0.226	0.320	0.357	0.455	0.431	0.145	0.149
DeepSAD	0.137	0.206	0.253	0.312	0.604	0.509	**0.762**	**0.686**	0.187	0.215
KDAlign-DeepSAD	**0.201**	**0.252**	**0.420**	**0.462**	**0.617**	**0.535**	0.731	0.637	**0.207**	**0.248**
REPEN	0.116	0.039	0.452	0.473	**0.726**	0.648	0.605	0.589	**0.245**	**0.283**
KDAlign-REPEN	**0.289**	**0.290**	**0.631**	**0.559**	0.720	**0.658**	**0.608**	**0.606**	0.181	0.204
DevNet	0.250	0.316	0.266	0.258	0.647	**0.543**	0.416	0.420	0.186	0.211
KDAlign-DevNet	**0.487**	**0.626**	**0.490**	**0.516**	**0.676**	0.533	**0.517**	**0.526**	**0.195**	**0.218**
PReNet	0.580	0.574	0.602	0.591	0.331	0.303	0.848	0.783	0.174	0.200
KDAlign-PReNet	**0.728**	**0.716**	**0.671**	**0.624**	**0.677**	**0.604**	**0.850**	0.783	**0.181**	**0.205**
FeaWAD	0.779	0.768	0.622	0.591	0.322	0.418	0.749	0.620	0.184	0.220
KDAlign-FeaWAD	**0.789**	**0.794**	**0.664**	**0.624**	**0.601**	**0.555**	**0.776**	**0.734**	**0.216**	**0.247**
ResNet	0.770	0.729	0.566	0.612	0.352	0.384	0.756	0.706	0.183	0.203
KDAlign-ResNet	**0.848**	**0.768**	**0.659**	**0.656**	**0.604**	**0.594**	**0.770**	**0.734**	**0.209**	**0.262**

- **FeaWAD** [74]. A neural network based model that incorporates the network architecture of DAGMM [75] with the deviation loss of DevNet.
- **ResNet** [23]. ResNet-like architecture turns out to be a strong baseline [28].

Parameter And Implementation Details. Firstly, acquiring knowledge is essential. It is worth noticing that the five datasets do not provide rules, and due to industrial security and privacy issues, obtaining well-defined rules directly is challenging. Therefore, we need to simulate the rules of these datasets to acquire knowledge. In our experiments, we train several decision tree models for each dataset using additional labels, and then extract the decision paths from the decision tree models as our if/else rules. In WSAD, anomaly samples are unbalanced and important, so we focus on the decision paths used for anomaly samples. A more detailed description of knowledge acquisition can be referred to the appendix. Secondly, we divide each dataset into a training set, a validation set, and a test set according to the scale of 7:1:2. To ensure that the rules really provide extra information (e.g., unseen anomaly scenarios) to supplement limited labeled samples, we delete the anomaly samples that match rules from the training set. Besides, for each training set, we only retain 10 labeled anomaly samples, treating the rest of the anomalies and all normal samples as unlabeled data, with the default label being normal samples. Besides, we also consider another three training settings with 1, 3, and 5 labeled anomaly samples.

Our implementation of SVM, KNN, and DT is consistent with the APIs of Sklearn [50]. We keep the default settings of SVM, KNN, and DT given by Sklearn. For representative WSAD methods, DeepSAD, REPEN, DevNet, PReNet, and FeaWAD are consistent with the Benchmark DeepOD [67], and ResNet is implemented based on the design for AD from [23]. The default optimizer of each baseline is Adam [32]. To apply our proposed KDAlign framework, we make slight adjustments to the representative WSAD methods. Concretely, during the forward propagation of these methods, in addition to returning the output of the final layer, they also return the sample hidden representations from the layer before the last one. All the models are tuned to the best performance on the validation set. Our codes are released at https://github.com/KDAlignForWWW2024/KDAlign.

4.2 Performance Comparison (RQ1)

Table 2 shows the model performance on 5 datasets w.r.t AUCPR and F1@K. Each dataset contains 10 labeled anomalies. Above all, we verify the effectiveness of the KDAlign framework on various deep learning-based WSAD baselines. The KDAlign based AD methods we proposed generally outperform the corresponding baselines.

Specifically, we have the following observations:

- We find that typical anomaly detection methods, including KNN, SVM, and DT, struggle when the number of labeled anomalies is extremely sparse. The SVM method shows good results on the Cardiotocography dataset, which might be coincidental.
- We observe that while representative WSAD methods demonstrate impressive performance on certain datasets, they invariably have weak performance on one or more datasets. For instance, DeepSAD outperforms most baselines on the SpamBase dataset but underperforms on the Amazon dataset. Based on the characteristics of these five datasets, the discrepancy may be due to the higher feature count in SpamBase and the lower feature

Table 3: Performance comparison between representative baselines and KDAlign under the setting of 1, 3, or 5 labeled anomalies w.r.t AUPRC. '-' indicates that the PReNet model can not handle setting of only 1 labeled anomaly samples.

Model	Amazon			Cardio			Satellite			SpamBase			YelpChi		
	1	3	5	1	3	5	1	3	5	1	3	5	1	3	5
KNN	0.065	0.065	0.080	0.236	0.253	0.286	0.323	0.319	0.319	0.416	0.416	0.414	0.145	0.145	0.145
SVM	0.238	0.124	0.093	0.290	0.304	0.293	0.349	0.305	0.313	0.437	0.425	0.536	0.148	0.150	0.165
DT	0.065	0.065	0.113	0.229	0.244	0.286	0.318	0.318	0.318	0.426	0.429	0.433	0.145	0.145	0.145
DevNet	0.128	0.103	0.135	0.267	0.269	0.286	**0.722**	**0.717**	**0.725**	0.416	0.416	0.416	**0.167**	0.169	0.169
KDAlign-DevNet	**0.739**	**0.747**	**0.570**	**0.528**	**0.436**	**0.550**	0.474	0.694	0.686	**0.489**	**0.461**	**0.494**	0.156	**0.200**	**0.195**
PReNet	-	0.152	0.488	-	0.390	0.626	-	0.344	0.266	-	0.689	**0.819**	-	0.164	0.161
KDAlign-PReNet	-	**0.617**	**0.623**	-	**0.656**	0.558	-	**0.748**	**0.767**	-	**0.741**	0.817	-	**0.176**	**0.207**
DeepSAD	0.129	0.070	0.104	0.355	0.248	0.259	**0.732**	**0.739**	0.670	**0.710**	0.668	0.602	0.188	0.199	0.197
KDAlign-DeepSAD	**0.347**	**0.514**	**0.271**	**0.639**	**0.480**	**0.517**	0.717	0.722	**0.735**	0.699	**0.778**	**0.779**	**0.205**	**0.208**	**0.215**
REPEN	0.116	0.116	0.116	0.452	0.452	0.452	0.730	0.730	0.730	0.608	0.608	0.608	**0.245**	**0.244**	**0.245**
KDAlign-REPEN	**0.289**	**0.289**	**0.289**	**0.630**	**0.630**	**0.630**	**0.741**	**0.741**	**0.741**	**0.631**	**0.631**	**0.631**	0.181	0.180	0.209
FeaWAD	0.692	0.274	0.734	0.545	**0.527**	**0.622**	0.582	0.570	0.686	**0.697**	0.717	0.756	0.170	0.177	0.212
KDAlign-FeaWAD	**0.738**	**0.611**	**0.778**	**0.654**	0.489	0.551	**0.751**	**0.769**	0.529	0.615	**0.765**	**0.775**	**0.212**	**0.193**	**0.240**
ResNet	0.785	0.629	0.777	0.590	**0.663**	**0.700**	0.328	0.359	0.353	**0.625**	0.601	0.637	0.183	0.175	0.175
KDAlign-ResNet	**0.805**	**0.744**	**0.834**	**0.642**	0.613	0.691	**0.696**	**0.676**	**0.699**	0.601	**0.621**	**0.668**	**0.201**	**0.207**	**0.207**

Table 4: AUPRC and F1@K results of Ablation Study. KD- represents the WSAD method incorporated knowledge without knowledge-data alignment.

Labeled Anomalies	Model	Amazon		Cardio		Satellite		SpamBase		YelpChi	
		PRC	F1@K	PRC	F1@K	PRC	F1@K	PRC	F1@K	PRC	F1@K
1	KD-ResNet	0.792	0.793	0.546	0.559	0.581	0.444	0.538	0.588	0.161	0.187
	KDAlign-ResNet	**0.805**	**0.800**	**0.642**	**0.581**	**0.696**	**0.575**	**0.601**	**0.643**	**0.201**	**0.266**
3	KD-ResNet	0.643	0.651	**0.629**	0.612	0.560	0.422	0.595	0.565	0.156	0.188
	KDAlign-ResNet	**0.744**	**0.742**	0.613	**0.645**	**0.676**	**0.592**	**0.621**	**0.654**	**0.207**	**0.261**
5	KD-ResNet	0.812	0.780	0.682	**0.667**	0.517	0.410	0.600	0.645	0.168	0.194
	KDAlign-ResNet	**0.834**	**0.806**	**0.691**	0.645	**0.699**	**0.577**	**0.668**	**0.694**	**0.207**	**0.263**
10	KD-ResNet	0.715	0.767	0.633	0.612	0.485	0.506	0.706	0.700	0.171	0.191
	KDAlign-ResNet	**0.848**	**0.768**	**0.659**	**0.656**	**0.604**	**0.594**	**0.770**	**0.734**	**0.209**	**0.262**
Average	KD-ResNet	0.741	0.748	0.623	0.613	0.536	0.446	0.610	0.625	0.164	0.190
	KDAlign-ResNet	**0.808**	**0.779**	**0.651**	**0.632**	**0.669**	**0.585**	**0.665**	**0.681**	**0.206**	**0.263**

count in the Amazon dataset. This is because DeepSAD focuses on anomaly feature representation learning [29]. REPEN method outperforms all other methods on the YelpChi dataset, but falls short on both the Amazon and Cardiotocography datasets. We surmise that this is because REPEN is an unsupervised anomaly feature representation learning method [29], and datasets like Amazon and Cardiotocography neither offer as many samples as YelpChi nor as many features as Satellite and SpamBase. The performance of the DevNet method on the Amazon, Cardiotocography, and SpamBase datasets is not satisfactory. This is mainly because the labeled anomalies available for these three datasets

cover a limited range of anomaly scenarios. As the DevNet approach focuses on Anomaly Score Learning [29], the scores it learns fail to distinguish between normal and anomalous samples.

- We find that methods like PReNet and FeaWAD, both belonging to the anomaly score learning [29], generally outperform DevNet and other baseline methods across all datasets. We attribute this promising performance primarily to the design of the PReNet and FeaWAD. PReNet method takes anomaly-anomaly, anomaly-unlabeled, and unlabeled-unlabeled instance pairs as input, and learns pairwise anomaly scores by discriminating these three types of linear pairwise interactions. This is an augmentation process of data distribution for existing labeled anomalies, which

subsequently aids in the learning of the final anomaly scores. The autoencoder architecture of FeaWAD is capable of mapping limited labeled samples to a latent space, thereby extending the distribution of these sparsely labeled anomalies and improving the learned Score distributions.

- We observe that our proposed KDAlign framework consistently enhances the performance of representative WSAD methods. For example, the KDAlign-PReNet method exhibits a 104.53% improvement over PReNet on the Satellite dataset, climbing from the last rank (excluding typical AD methods) to the second rank. In addition, DeepSAD, REPEN and DevNet, which introduced KDAlign, also have nearly doubled improvements on the Amazon and Cardiotocography data sets. Even when FeaWAD and ResNet already demonstrate commendable results, the KDAlign framework still manages to further boost their performance. In some isolated cases, KDAlign fails to enhance the performance of baseline methods. The reason may be that the unseen anomalies learned by the original baseline methods overlap with the anomalies covered by knowledge, and aligning them might distort the original data representation.
- We find that the best-performing methods on each dataset are based on the KDAlign framework. This indicates that KDAlign can not only improve the performance of baseline methods but also holds the potential to provide new state-of-the-art results in weakly supervised settings.

In addition, we also use Table 3 to present the experimental results of KDAlign and representative baselines with respect to AUCPR when the number of labeled anomalies is 1, 3, or 5. The results for F1@K will be shown in the appendix.

4.3 Ablation Study (RQ2)

We present the results of our Ablation Study in Table 4, with respect to AUPRC and F1@K. Concretely, we compare the model performance of KDAlign-ResNet and KD-ResNet across five datasets under four WSAD settings, where the KD-ResNet introduces knowledge without the knowledge-data alignment and the label anomalies of each dataset are respectively 1,3,5 and 10. According to the experimental results, we can clearly find that KDAlign-ResNet outperforms KD-ResNet in almost all settings. Besides, we observe that the standard deviation of KDAlign-ResNet across the four settings is significantly lower than that of KD-ResNet. This suggests that the performance of KDAlign-ResNet remains relatively consistent as the number of labeled samples varies from 1 to 10, reflecting the robustness of the KDAlign framework.
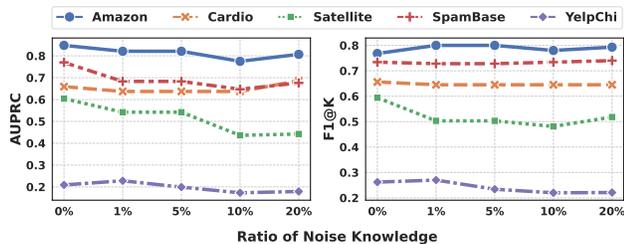

Figure 3: Noisy knowledge study on KDAlign-ResNet.

4.4 Impact of Noisy Knowledge (RQ3)

We use Figure 3 to illustrate the impact of noisy knowledge on the performance of KDAlign-ResNet. By 'noisy knowledge', we refer to the incompletely correct rules that will incorrectly judge some samples, leading to detection errors. Specifically, we investigate the performance of KDAlign-ResNet across five datasets under four noisy settings. The ratio of noise knowledge pertains to the ratio of incompletely correct rules to the total rules. From our experiments, we make the following observations: Compared to the setting without noise, we find that as the ratio increases, the performance of KDAlign-ResNet does not fluctuate significantly, except for the Satellite dataset. The reason might be the knowledge with noise happens to cover some unseen important anomaly scenarios, which in turn results in a decline in model performance. It is worth noting that compared with Table 2, even when impacted by noisy knowledge, the performance of KDAlign-ResNet remains superior to that of ResNet.

5 RELATED WORK

5.1 Weakly Supervised Anomaly Detection

Weakly supervised anomaly detection aims to train an effective AD model with limited labeled anomaly samples and extensive unlabeled data. Early studies [45, 53, 54] on WSAD primarily involved designing a feature extractor based on unsupervised AD algorithms and then learning a supervised classifier using labeled data such as eepSAD [54] and REPEN [45]. Recent studies [37, 41, 47, 74] focus on designing end-to-end deep framework. For example, DevNet [48] utilizes a prior probability and a margin hyperparameter to enforce obvious deviations in anomaly scores between normal and abnormal data. FeaWAD [74] incorporates the DAGMM [75] network architecture with the deviation loss. PReNet [47] formulates the scoring function as a pairwise relation learning task.

Another research line utilizes active learning or reinforcement learning to reduce the cost of obtaining anomaly labels. For instance, AAD [16] leverages the active learning technique, which operates in an interactive loop for data exploration and maximizes the total number of true anomalies presented to the expert under a query budget. DPLAN [49] considers simultaneously exploring both limited labeled anomaly examples and scarce unlabeled anomalies to extend the learned abnormality, leading to the joint optimization of both objectives.

In contrast to above studies, our work introduces rule knowledge to supplement the limited anomaly samples. Similar to label annotations, such knowledge also contains human supervision, but has been largely overlooked.

5.2 Neural-symbolic Systems

The symbolic system excels in leveraging knowledge, while the neural system is adept at harnessing data. Both knowledge and data play a pivotal role in decision-making processes. There is a burgeoning interest among AI researchers to fuse the symbolic and neural paradigms, aiming to harness the strengths of both [19, 20, 30, 56, 65]. When juxtaposing neural-symbolic systems against purely neural or symbolic ones, three aspects come to the fore [68].

First is the Efficiency. Neural-symbolic models can expedite computations, making them suitable for reasoning on vast data sets. Second is the Generalization. These systems are not solely reliant on extensive labeled datasets, endowing them with impressive generalization capabilities. By integrating expert or background knowledge, neural-symbolic models can compensate for sparse training data, achieving commendable performance without sacrificing generalizability. Third is the interpretability. Neural-symbolic architectures offer transparency in their reasoning, enhancing their interpretability [68]. Such transparency is invaluable in fields like medical image analysis, where stakeholders require both the outcome and an understanding of the decision-making rationale [68]. In general, the neural-symbolic system is a promising approach to effectively simultaneously leverage knowledge and data for decision-making processes. However, its potential in weakly supervised anomaly detection has yet to be explored.

6 CONCLUSION AND FUTURE WORK

In this paper, we study the problem of weakly supervised anomaly detection and propose a novel WSAD framework named KDAlign, which reformulates knowledge incorporation as knowledge-data alignment, adopts OT for effectively resolving knowledge-data alignment, and finally supplements the limited anomaly samples to improve the performance of WSAD models. We extensively conduct experiments on five real-world datasets and the experimental results demonstrate that our framework outperforms the other competitors.

For the future, we plan to extend our work in following directions: (1) Extend to graph domain [29]; (2) Introduce other OT methods, such as [61]; (3) Improve explainability.

ACKNOWLEDGMENTS

REFERENCES

[1] Samet Akcay, Amir Atapour-Abarghouei, and Toby P Breckon. 2019. Ganomaly: Semi-supervised anomaly detection via adversarial training. In *Computer Vision–ACCV 2018: 14th Asian Conference on Computer Vision, Perth, Australia, December 2–6, 2018, Revised Selected Papers, Part III 14.* Springer, 622–637.

[2] Diogo Ayres-de Campos, Joao Bernardes, Antonio Garrido, Joaquim Marques-de Sa, and Luis Pereira-Leite. 2000. SisPorto 2.0: a program for automated analysis of cardiotocograms. *Journal of Maternal-Fetal Medicine* 9, 5 (2000), 311–318.

[3] Gary Bécigneul, Octavian-Eugen Ganea, Benson Chen, Regina Barzilay, and Tommi S Jaakkola. 2020. Optimal transport graph neural networks. In *International Conference on Learning Representations*.

[4] WANG Botao, Jia Li, Yang Liu, Jiashun Cheng, Yu Rong, Wenjia Wang, and Fugee Tsung. 2023. Deep Insights into Noisy Pseudo Labeling on Graph Data. In *Thirty-seventh Conference on Neural Information Processing Systems*.

[5] Yacine Bouzida and Frederic Cuppens. 2006. Neural networks vs. decision trees for intrusion detection. In *IEEE/IST workshop on monitoring, attack detection and mitigation (MonAM)*, Vol. 28. 29.

[6] L Breiman, JH Friedman, RA Olshen, and CJ Stone. 1984. Classification and regression trees (Wadsworth, Belmont, CA). *ISBN-13* (1984), 978–0412048418.

[7] Dawei Cheng, Yujia Ye, Sheng Xiang, Zhenwei Ma, Ying Zhang, and Changjun Jiang. 2023. Anti-Money Laundering by Group-Aware Deep Graph Learning. *IEEE Transactions on Knowledge and Data Engineering* (2023).

[8] Marco Console, Paolo Guagliardo, and Leonid Libkin. 2022. Propositional and predicate logics of incomplete information. *Artificial Intelligence* 302 (2022), 103603. https://doi.org/10.1016/j.artint.2021.103603

[9] Corinna Cortes and Vladimir Vapnik. 1995. Support vector machine. *Machine learning* 20, 3 (1995), 273–297.

[10] Thomas Cover and Peter Hart. 1967. Nearest neighbor pattern classification. *IEEE transactions on information theory* 13, 1 (1967), 21–27.

[11] Marco Cuturi. 2013. Sinkhorn distances: Lightspeed computation of optimal transport. *Advances in neural information processing systems* 26 (2013).

[12] Adnan Darwiche. 2001. Decomposable negation normal form. *Journal of the ACM (JACM)* 48, 4 (2001), 608–647.

[13] Adnan Darwiche. 2001. On the tractable counting of theory models and its application to truth maintenance and belief revision. *Journal of Applied Non-Classical Logics* 11, 1-2 (2001), 11–34.

[14] Adnan Darwiche. 2004. New Advances in Compiling CNF to Decomposable Negation Normal Form. In *Proceedings of the 16th European Conference on Artificial Intelligence* (Valencia, Spain) *(ECAI'04)*. IOS Press, NLD, 318–322.

[15] Adnan Darwiche and Pierre Marquis. 2002. A knowledge compilation map. *Journal of Artificial Intelligence Research* 17 (2002), 229–264.

[16] Shubhomoy Das, Weng-Keen Wong, Thomas Dietterich, Alan Fern, and Andrew Emmott. 2016. Incorporating expert feedback into active anomaly discovery. In *2016 IEEE 16th International Conference on Data Mining (ICDM)*. IEEE, 853–858.

[17] Vilnis Detlovs and Karlis Podnieks. 2011. Introduction to Mathematical Logic. *University of Latvia* (2011).

[18] Kaize Ding, Qinghai Zhou, Hanghang Tong, and Huan Liu. 2021. Few-shot network anomaly detection via cross-network meta-learning. In *Proceedings of the Web Conference 2021*. 2448–2456.

[19] Paolo Dragone, Stefano Teso, and Andrea Passerini. 2021. Neuro-symbolic constraint programming for structured prediction. *arXiv preprint arXiv:2103.17232* (2021).

[20] Artur d'Avila Garcez, Sebastian Bader, Howard Bowman, Luis C Lamb, Leo de Penning, BV Illuminoo, Hoifung Poon, and COPPE Gerson Zaverucha. 2022. Neural-symbolic learning and reasoning: A survey and interpretation. *Neuro-Symbolic Artificial Intelligence: The State of the Art* 342, 1 (2022), 327.

[21] Zheng Ge, Songtao Liu, Zeming Li, Osamu Yoshie, and Jian Sun. 2021. Ota: Optimal transport assignment for object detection. In *Proceedings of the IEEE/CVF Conference on Computer Vision and Pattern Recognition*. 303–312.

[22] Aude Genevay, Marco Cuturi, Gabriel Peyré, and Francis Bach. 2016. Stochastic optimization for large-scale optimal transport. *Advances in neural information processing systems* 29 (2016).

[23] Yury Gorishniy, Ivan Rubachev, Valentin Khrulkov, and Artem Babenko. 2021. Revisiting deep learning models for tabular data. *Advances in Neural Information Processing Systems* 34 (2021), 18932–18943.

[24] Songqiao Han, Xiyang Hu, Hailiang Huang, Minqi Jiang, and Yue Zhao. 2022. Adbench: Anomaly detection benchmark. *Advances in Neural Information Processing Systems* 35 (2022), 32142–32159.

[25] Mark Hopkins, Erik Reeber, George Forman, and Jaap Suermondt. 1999. Spambase. UCI Machine Learning Repository. DOI: https://doi.org/10.24432/C53G6X.

[26] Chaoqin Huang, Fei Ye, Peisen Zhao, Ya Zhang, Yan-Feng Wang, and Qi Tian. 2020. Esad: End-to-end deep semi-supervised anomaly detection. *arXiv preprint arXiv:2012.04905* (2020).

[27] Jinglong Ji, Fujin Zhu, Jiaxu Cui, Haihong Zhao, and Bo Yang. 2022. A dual-system method for intelligent fault localization in communication networks. In *ICC 2022-IEEE International Conference on Communications*. IEEE, 4062–4067.

[28] Minqi Jiang, Songqiao Han, and Hailiang Huang. 2023. Anomaly Detection with Score Distribution Discrimination. In *Proceedings of the 29th ACM SIGKDD Conference on Knowledge Discovery and Data Mining*. 984–996.

[29] Minqi Jiang, Chaochuan Hou, Ao Zheng, Xiyang Hu, Songqiao Han, Hailiang Huang, Xiangnan He, Philip S Yu, and Yue Zhao. 2023. Weakly supervised anomaly detection: A survey. *arXiv preprint arXiv:2302.04549* (2023).

[30] Navdeep Kaur, Gautam Kunapuli, Tushar Khot, Kristian Kersting, William Cohen, and Sriraam Natarajan. 2018. Relational restricted boltzmann machines: A probabilistic logic learning approach. In *Inductive Logic Programming: 27th International Conference, ILP 2017, Orléans, France, September 4-6, 2017, Revised Selected Papers 27*. Springer, 94–111.

[31] Haider Adnan Khan, Nader Sehatbakhsh, Luong N Nguyen, Robert L Callan, Arie Yeredor, Milos Prvulovic, and Alenka Zajić. 2019. IDEA: Intrusion detection through electromagnetic-signal analysis for critical embedded and cyber-physical systems. *IEEE Transactions on Dependable and Secure Computing* 18, 3 (2019), 1150–1163.

[32] DP Kingma. 2015. Adam: a method for stochastic optimization. In *The 3rd International Conference on Learning Representations*.

[33] Thomas N. Kipf and Max Welling. 2017. Semi-Supervised Classification with Graph Convolutional Networks. In *International Conference on Learning Representations*.

[34] Kevin C. Klement. 2004. Propositional Logic. In *Internet Encyclopedia of Philosophy*.

[35] Meng-Chieh Lee, Yue Zhao, Aluna Wang, Pierre Jinghong Liang, Leman Akoglu, Vincent S Tseng, and Christos Faloutsos. 2020. Autoaudit: Mining accounting and time-evolving graphs. In *2020 IEEE International Conference on Big Data (Big Data)*. IEEE, 950–956.

[36] Jia Li, Zhichao Han, Hong Cheng, Jiao Su, Pengyun Wang, Jianfeng Zhang, and Lujia Pan. 2019. Predicting path failure in time-evolving graphs. In *Proceedings*

of the 25th ACM SIGKDD international conference on knowledge discovery & data mining. 1279–1289.

[37] Jia Li, Yongfeng Huang, Heng Chang, and Yu Rong. 2022. Semi-supervised hierarchical graph classification. *IEEE Transactions on Pattern Analysis and Machine Intelligence* 45, 5 (2022), 6265–6276.

[38] Jia Li, Yu Rong, Hong Cheng, Helen Meng, Wenbing Huang, and Junzhou Huang. 2019. Semi-supervised graph classification: A hierarchical graph perspective. In *The World Wide Web Conference*. 972–982.

[39] Xujia Li, Yuan Li, Xueying Mo, Hebing Xiao, Yanyan Shen, and Lei Chen. 2023. Diga: Guided Diffusion Model for Graph Recovery in Anti-Money Laundering. In *Proceedings of the 29th ACM SIGKDD Conference on Knowledge Discovery and Data Mining*. 4404–4413.

[40] Zhe Li, Chunhua Sun, Chunli Liu, Xiayu Chen, Meng Wang, and Yezheng Liu. 2022. Dual-MGAN: An Efficient Approach for Semi-supervised Outlier Detection with Few Identified Anomalies. *ACM Transactions on Knowledge Discovery from Data (TKDD)* 16, 6 (2022), 1–30.

[41] Zhe Li, Chunhua Sun, Chunli Liu, Xiayu Chen, Meng Wang, and Yezheng Liu. 2022. Dual-MGAN: An Efficient Approach for Semi-supervised Outlier Detection with Few Identified Anomalies. *ACM Transactions on Knowledge Discovery from Data (TKDD)* 16, 6 (2022), 1–30.

[42] Xiexiong Lin, Huaisong Li, Tao Huang, Feng Wang, Linlin Chao, Fuzhen Zhuang, Taifeng Wang, and Tianyi Zhang. 2022. A Logic Aware Neural Generation Method for Explainable Data-to-text. In *Proceedings of the 28th ACM SIGKDD Conference on Knowledge Discovery and Data Mining*. 3318–3326.

[43] Julian John McAuley and Jure Leskovec. 2013. From amateurs to connoisseurs: modeling the evolution of user expertise through online reviews. In *Proceedings of the 22nd international conference on World Wide Web*. 897–908.

[44] Danilo Motta, Wallace Casaca, and Afonso Paiva. 2019. Vessel optimal transport for automated alignment of retinal fundus images. *IEEE Transactions on Image Processing* 28, 12 (2019), 6154–6168.

[45] Guansong Pang, Longbing Cao, Ling Chen, and Huan Liu. 2018. Learning representations of ultrahigh-dimensional data for random distance-based outlier detection. In *Proceedings of the 24th ACM SIGKDD international conference on knowledge discovery & data mining*. 2041–2050.

[46] Guansong Pang, Choubo Ding, Chunhua Shen, and Anton van den Hengel. 2021. Explainable deep few-shot anomaly detection with deviation networks. *arXiv preprint arXiv:2108.00462* (2021).

[47] Guansong Pang, Chunhua Shen, Huidong Jin, and Anton van den Hengel. 2023. Deep weakly-supervised anomaly detection. In *Proceedings of the 29th ACM SIGKDD Conference on Knowledge Discovery and Data Mining*. 1795–1807.

[48] Guansong Pang, Chunhua Shen, and Anton van den Hengel. 2019. Deep anomaly detection with deviation networks. In *Proceedings of the 25th ACM SIGKDD international conference on knowledge discovery & data mining*. 353–362.

[49] Guansong Pang, Anton van den Hengel, Chunhua Shen, and Longbing Cao. 2021. Toward deep supervised anomaly detection: Reinforcement learning from partially labeled anomaly data. In *Proceedings of the 27th ACM SIGKDD conference on knowledge discovery & data mining*. 1298–1308.

[50] F. Pedregosa, G. Varoquaux, A. Gramfort, V. Michel, B. Thirion, O. Grisel, M. Blondel, P. Prettenhofer, R. Weiss, V. Dubourg, J. Vanderplas, A. Passos, D. Cournapeau, M. Brucher, M. Perrot, and E. Duchesnay. 2011. Scikit-learn: Machine Learning in Python. *Journal of Machine Learning Research* 12 (2011), 2825–2830.

[51] J. Ross Quinlan. 1987. Simplifying decision trees. *International journal of man-machine studies* 27, 3 (1987), 221–234.

[52] Shebuti Rayana and Leman Akoglu. 2015. Collective opinion spam detection: Bridging review networks and metadata. In *Proceedings of the 21th acm sigkdd international conference on knowledge discovery and data mining*. 985–994.

[53] Lukas Ruff, Robert Vandermeulen, Nico Goernitz, Lucas Deecke, Shoaib Ahmed Siddiqui, Alexander Binder, Emmanuel Müller, and Marius Kloft. 2018. Deep one-class classification. In *International conference on machine learning*. PMLR, 4393–4402.

[54] Lukas Ruff, Robert A Vandermeulen, Nico Görnitz, Alexander Binder, Emmanuel Müller, Klaus-Robert Müller, and Marius Kloft. 2019. Deep Semi-Supervised Anomaly Detection. In *International Conference on Learning Representations*.

[55] John Sipple. 2020. Interpretable, multidimensional, multimodal anomaly detection with negative sampling for detection of device failure. In *International Conference on Machine Learning*. PMLR, 9016–9025.

[56] Gustav Sourek, Vojtech Aschenbrenner, Filip Zelezny, Steven Schockaert, and Ondrej Kuzelka. 2018. Lifted relational neural networks: Efficient learning of latent relational structures. *Journal of Artificial Intelligence Research* 62 (2018), 69–100.

[57] Ashwin Srinivasan. 1993. Statlog (Landsat Satellite). UCI Machine Learning Repository. DOI: https://doi.org/10.24432/C55887.

[58] Xiangguo Sun, Hong Cheng, Jia Li, Bo Liu, and Jihong Guan. 2023. All in One: Multi-Task Prompting for Graph Neural Networks. In *Proceedings of the 26th ACM SIGKDD international conference on knowledge discovery & data mining (KDD'23)*. 2120–2131.

[59] Jianheng Tang, Fengrui Hua, Ziqi Gao, Peilin Zhao, and Jia Li. 2023. GADBench: Revisiting and Benchmarking Supervised Graph Anomaly Detection. In *Thirty-seventh Conference on Neural Information Processing Systems*.

[60] Jianheng Tang, Jiajin Li, Ziqi Gao, and Jia Li. 2022. Rethinking graph neural networks for anomaly detection. In *International Conference on Machine Learning*. PMLR, 21076–21089.

[61] Jianheng Tang, Weiqi Zhang, Jiajin Li, Kangfei Zhao, Fugee Tsung, and Jia Li. 2023. Robust Attributed Graph Alignment via Joint Structure Learning and Optimal Transport. In *2023 IEEE 39th International Conference on Data Engineering (ICDE)*. 1638–1651. https://doi.org/10.1109/ICDE55515.2023.00129

[62] Jianheng Tang, Kangfei Zhao, and Jia Li. 2023. A Fused Gromov-Wasserstein Framework for Unsupervised Knowledge Graph Entity Alignment. In *Findings of the Association for Computational Linguistics: ACL 2023*. Toronto, Canada, 3320–3334. https://doi.org/10.18653/v1/2023.findings-acl.205

[63] Bowen Tian, Qinliang Su, and Jian Yin. 2022. Anomaly detection by leveraging incomplete anomalous knowledge with anomaly-aware bidirectional gans. *arXiv preprint arXiv:2204.13335* (2022).

[64] Fuying Wang, Yuyin Zhou, Shujun Wang, Varut Vardhanabhuti, and Lequan Yu. 2022. Multi-granularity cross-modal alignment for generalized medical visual representation learning. *Advances in Neural Information Processing Systems* 35 (2022), 33536–33549.

[65] Yaqi Xie, Ziwei Xu, Mohan S Kankanhalli, Kuldeep S Meel, and Harold Soh. 2019. Embedding symbolic knowledge into deep networks. *Advances in neural information processing systems* 32 (2019).

[66] Yaqi Xie, Ziwei Xu, Kuldeep S Meel, Mohan S Kankanhalli, and Harold Soh. 2019. Embedding Symbolic Knowledge into Deep Networks. In *NeurIPS*.

[67] Hongzuo Xu, Guansong Pang, Yijie Wang, and Yongjun Wang. 2023. Deep Isolation Forest for Anomaly Detection. *IEEE Transactions on Knowledge and Data Engineering* (2023), 1–14. https://doi.org/10.1109/TKDE.2023.3270293

[68] Dongran Yu, Bo Yang, Dayou Liu, Hui Wang, and Shirui Pan. 2023. A survey on neural-symbolic learning systems. *Neural Networks* (2023).

[69] Zhichen Zeng, Si Zhang, Yinglong Xia, and Hanghang Tong. 2023. PARROT: Position-Aware Regularized Optimal Transport for Network Alignment. In *Proceedings of the ACM Web Conference 2023*. 372–382.

[70] Daochen Zha, Kwei-Herng Lai, Mingyang Wan, and Xia Hu. 2020. Meta-AAD: Active anomaly detection with deep reinforcement learning. In *2020 IEEE International Conference on Data Mining (ICDM)*. IEEE, 771–780.

[71] Linhao Zhang, Li Jin, Xian Sun, Guangluan Xu, Zequn Zhang, Xiaoyu Li, Nayu Liu, Qing Liu, and Shiyao Yan. 2023. TOT: Topology-Aware Optimal Transport for Multimodal Hate Detection. In *Proceedings of the AAAI Conference on Artificial Intelligence*, Vol. 37. 4884–4892.

[72] Weiqi Zhang, Jianfeng Zhang, Jia Li, and Fugee Tsung. 2023. A Co-training Approach for Noisy Time Series Learning *(CIKM '23)*. Association for Computing Machinery, New York, NY, USA, 3308–3318. https://doi.org/10.1145/3583780.3614759

[73] Haihong Zhao, Bo Yang, Jiaxu Cui, Qianli Xing, Jiaxing Shen, Fujin Zhu, and Jiannong Cao. 2023. Effective Fault Scenario Identification for Communication Networks Via Knowledge-Enhanced Graph Neural Networks. *IEEE Transactions on Mobile Computing* (2023), 1–16. https://doi.org/10.1109/TMC.2023.3271715

[74] Yingjie Zhou, Xucheng Song, Yanru Zhang, Fanxing Liu, Ce Zhu, and Lingqiao Liu. 2021. Feature encoding with autoencoders for weakly supervised anomaly detection. *IEEE Transactions on Neural Networks and Learning Systems* 33, 6 (2021), 2454–2465.

[75] Bo Zong, Qi Song, Martin Renqiang Min, Wei Cheng, Cristian Lumezanu, Daeki Cho, and Haifeng Chen. 2018. Deep autoencoding gaussian mixture model for unsupervised anomaly detection. In *International conference on learning representations*.

A KNOWLEDGE ACQUISITION

Rule knowledge usually widely exists in industry [73]. However, hindered by concerns for industrial safety and privacy, procuring traditional rule knowledge from the industry poses challenges. Therefore, it is necessary to find an alternate way to simulate the industrial rule knowledge. We find the decision tree method is a promising way [5, 51], where every decision path can be regarded as a rule knowledge. First, the representation format of decision paths is the same as industrial rule knowledge, often manifesting as if/else statements. Second, decision paths are conveniently accessible—for instance, we can extract decision paths from well-trained decision trees.

Specifically, referring to Fig. 4, we assign three steps to acquire rule knowledge based on decision tree models: **Step 1:** Given a collection of m samples $\mathbf{X} = \{x_1, ..., x_m\} \in \mathbb{R}^{m \times d}$ and the binary ground truth labels $\mathbf{y} = \{y_1, ..., y_m\} \in \{0, 1\}^m$, we train r decision trees; **Step 2:** For the r trained decision trees, we extract *all-right anomaly paths* (knowledge set) $\mathbf{R} = \{r_1, ..., r_s\}$ included in them as the rule knowledge. An *all-right anomaly path* means that the labels of specific samples in $\mathbf{X}$ passing the decision path are all anomalous.
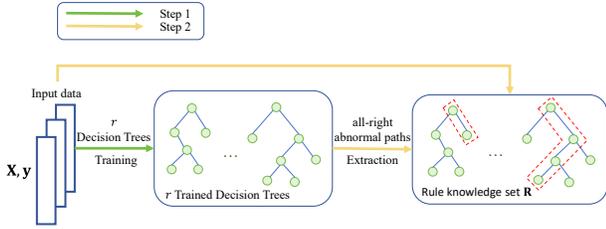

Figure 4: Knowledge Acquisition: Using decision trees to simulate industrial rule knowledge.

B KNOWLEDGE ENCODER

Preliminaries: This is a brief introduction to d-DNNF, which is used in Knowledge Encoder. A formula that is a conjunction of clauses (a disjunction of literals) is in the Conjunctive Normal Form (CNF). Let S be the set of propositional variables. A sentence in Negation Normal Form (NNF) is defined as a rooted directed acyclic graph (DAG) where each leaf node is labeled with True, False, $s, or \neg s, s \in S$; and each internal node is labeled with $\wedge$ or $\vee$ and can have discretionarily many children. Deterministic Decomposable Negation Normal Form (d-DNNF) [13, 15] further imposes that the representation is: (i) **Deterministic**: An NNF is deterministic if the operands of $\vee$ in all well-formed boolean formula in NNF are mutually inconsistent; (ii) **Decomposable**: An NNF is decomposable if the operands of $\wedge$ in all well-formed boolean formula in the NNF are expressed on a mutually disjoint set of variables. Opposite to CNF and more general forms, d-DNNF has many satisfactory tractability properties (e.g., polytime satisfiability and polytime model counting). Because of having tractability properties, it is appealing for complex AI applications to adopt d-DNNF [12].

In the paper, we mentioned the use of a **Knowledge Encoder** module to map propositional formulae into an embedding space. Concretely, we utilize the d-DNNF graph structure to represent

a propositional formula f_i and then apply a multi-layer Graph Convolutional Network [33] as an encoder to project the formula, f_i. In the following paragraphs, we further detail the **Knowledge Encoder** module. Note that the **Knowledge Encoder** $\phi_F(\cdot)$ is trained before KDAlign framework.

The input for training $\phi_F(\cdot)$ consists of specialized d-DNNF graphs which contribute to enhanced symbolic (knowledge) embeddings. These graphs are built from formulae that have been restructured based on decision paths. To construct the specific graphs based on these formulae, we first change the formulae in CNF and then use **c2d** to compile these formulae in d-DNNF [13–15]. For example, based on Formula '$p_1 \wedge p_2 \Rightarrow q$' in Section 3.2, we construct a CNF expression by Formula. (7). Then, after executing **c2d**, Formula. (7) can be expressed in d-DNNF shown by Formula. (8).

$$\neg p_1 \vee \neg p_2 \vee q \tag{7}$$

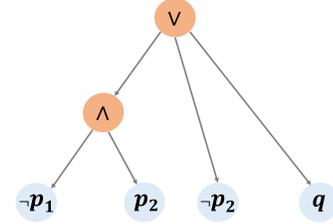$$(\neg p_1 \wedge p_2) \vee \neg p_2 \vee q \tag{8}$$

Figure 5: The d-DNNF graph structure generated based on Formula. (8).

Then a propositional formula can be represented as a directed or undirected graph $G = (V, E)$, consisting of N nodes denoted by $v_i \in V$ and edges represented as $(v_i; v_j) \in E$. Individual nodes are either propositions (leaf nodes) or logical operators ($\wedge; \vee; \Longrightarrow$), where propositions are connected to their respective operators. Fig. 5 can help understand the concrete structure. In addition to the mentioned nodes, every graph, like Fig. 5, is further augmented by a global node linked to all other nodes. In $\phi_F(\cdot)$, the graphs are regarded as undirected graphs.

The layer-wise propagation rule of GCN is,

$$Z^{(l+1)} = \sigma(\tilde{D}^{-\frac{1}{2}} \tilde{A} \tilde{D}^{-\frac{1}{2}} Z^{(l)} W^{(l)}) \tag{9}$$

where $Z^{(l+1)}$ represent the learnt latent node embeddings at l^{th} (note that $Z^{(0)} = X$), $\tilde{A} = A + I_N$ represents the adjacency matrix of the undirected graph G with added self-connections through the identity matrix I_N. $\tilde{D}$ is a diagonal degree matrix with $\tilde{D}_{ii} = \sum_j \tilde{A}_{ij}$. The weight matrices for layer-specific training are $W^{(l)}$, and $\sigma(\cdot)$ represents the activation function. To more effectively capture the semantics conveyed through the graphs, the $\phi_F(\cdot)$ function incorporates two additional adjustments: heterogeneous node embeddings and semantic regularization, as cited in [66]. The concrete code implementation is accessible at https://github.com/ZiweiXU/LENSR.

Haihong Zhao, Chenyi Zi, Yang Liu, Chen Zhang, Yan Zhou, and Jia Li[*]

Table 5: Performance comparison between representative baselines and KDAlign under the setting of 1, 3, or 5 labeled anomalies w.r.t F1@K. '-' indicates that the PReNet model can not handle the setting of only 1 labeled anomaly sample.

Model	Amazon			Cardio			Satellite			SpamBase			YelpChi		
	1	3	5	1	3	5	1	3	5	1	3	5	1	3	5
KNN	0.052	0.045	0.071	0.204	0.215	0.226	0.357	0.357	0.357	0.420	0.417	0.411	0.150	0.149	0.149
SVM	0.045	0.026	0.026	0.269	0.280	0.215	0.308	0.279	0.318	0.431	0.386	0.440	0.162	0.153	0.171
DT	0.052	0.052	0.097	0.194	0.194	0.226	0.355	0.357	0.355	0.426	0.426	0.420	0.150	0.150	0.150
DevNet	0.180	0.116	0.123	0.247	0.269	0.258	**0.555**	0.557	**0.562**	0.420	0.423	0.423	**0.181**	0.185	0.184
KDAlign-DevNet	**0.735**	**0.709**	**0.638**	**0.528**	**0.436**	**0.516**	0.459	**0.559**	0.547	**0.489**	**0.461**	**0.494**	0.156	**0.200**	**0.195**
PReNet	-	0.277	0.568	-	0.419	0.581	-	0.386	0.244	-	0.669	0.754	-	0.173	0.194
KDAlign-PReNet	-	**0.658**	**0.600**	-	**0.634**	**0.591**	-	**0.597**	0.641	-	**0.703**	0.749	-	**0.221**	**0.224**
DeepSAD	0.110	0.077	0.161	0.387	0.258	0.247	0.582	0.577	0.548	0.651	0.629	0.594	0.209	0.221	0.221
KDAlign-DeepSAD	**0.355**	**0.484**	**0.368**	**0.624**	**0.495**	**0.581**	**0.641**	**0.611**	**0.643**	**0.706**	**0.723**	**0.689**	**0.230**	**0.248**	**0.259**
REPEN	0.039	0.039	0.039	0.473	0.473	0.473	0.655	0.655	0.655	0.589	0.589	0.589	**0.283**	**0.282**	**0.283**
KDAlign-REPEN	**0.290**	**0.290**	**0.290**	**0.559**	**0.559**	**0.559**	**0.658**	**0.658**	**0.658**	**0.608**	**0.608**	**0.608**	0.181	0.180	0.209
FeaWAD	0.677	0.368	0.710	0.570	**0.548**	**0.656**	0.472	0.457	**0.538**	**0.677**	0.703	0.726	0.199	0.204	0.235
KDAlign-FeaWAD	**0.729**	**0.677**	**0.774**	**0.602**	0.505	0.581	**0.623**	**0.650**	0.501	0.640	**0.754**	**0.740**	**0.245**	**0.228**	**0.266**
ResNet	0.781	0.658	0.774	**0.602**	0.645	**0.677**	0.340	0.369	0.369	0.620	0.586	0.603	0.195	0.190	0.207
KDAlign-ResNet	**0.800**	**0.742**	**0.806**	0.581	0.645	0.645	**0.575**	**0.592**	**0.577**	**0.643**	**0.654**	**0.694**	**0.266**	**0.261**	**0.263**

Table 6: Optimal Parameter of KDAlign-FeaWAD

Dataset Name	Epoch	Layers	Learning Rate	Hidden Dimension	Rule Weight	Activation
Amazon	20	2	0.001	32	0.01	ReLU
Cardiotocography	20	2	0.01	32	0.01	ReLU
Satellite	20	3	0.001	64	0.05	ReLU
SpamBase	20	3	0.001	64	0.05	ReLU
YelpChi	100	2	0.01	32	0.05	ReLU

Table 7: Optimal Parameter of KDAlign-ResNet

Dataset Name	Epoch	Learning Rate	Blocks	Hidden Dimension	Rule Deight	Main Dimension	Dropout First	Dropout Second
Amazon	50	0.01	3	256	0.1	192	0.2	0
Cardiotocography	50	0.01	3	128	0.01	64	0.2	0
Satellite	200	0.01	3	128	3	128	0.2	0
SpamBase	50	0.01	2	128	0.01	64	0.2	0
YelpChi	50	0.01	3	256	3	64	0.2	0

C   IMPLEMENTATION DETAILS

Hardware Specifications. All our experiments were carried out on a Linux server equipped with AMD EPYC 7763 64-Core Processor, 503GB RAM, and eight NVIDIA RTX4090 GPUs with a total of 192G memory.

Hyperparameter Settings. Table 6 and Table 7 respectively show our optimal hyperparameter settings of KDAlign-FeaWAD and KDAlign-ResNet utilized in our experiments clearly, which are trained on 10 labeled anomaly samples.